

Radio luminosity of GLEAM-X J162759.5-523504.3: does it really exceed the spin-down power of the pulsar?

M. Hakan Erkut¹★

¹*Feza Gürsey Center for Physics and Mathematics, Boğaziçi University, 34684, Istanbul, Turkey*

Accepted XXX. Received YYY; in original form ZZZ

ABSTRACT

The recently discovered radio pulsar GLEAM-X J162759.5-523504.3 with an extremely long spin period was reported to have a radio luminosity that exceeds by orders of magnitude the spin-down power of the pulsar. In this Letter, we rigorously calculate the radio luminosity of the source taking into account the dependence of the opening angle of the pulsar-emission cone first on the spin period alone and then on both the spin parameters and the observing frequency. We also revise the value of the spin-down power reported previously. Our analysis is based on the description of the spectral data in terms of two power-law indices as well as a single power-law index. Even if the pulsar’s opening angle is treated as a frequency-independent parameter in line with the usual assumption, the period dependence of this parameter implies relatively small opening angles and therefore radio luminosities well below the spin-down power. Although we estimate higher radio luminosities in the physically more plausible case of a frequency-dependent opening angle, the spin-down power is again not exceeded by the highest possible radio luminosity. The radio efficiency of GLEAM-X J162759.5-523504.3 can therefore not be used in favour of a magnetar hypothesis.

Key words: pulsars: individual: GLEAM-X J162759.5-523504.3 – stars: magnetars – stars: neutron – radio continuum: transients

1 INTRODUCTION

The rotational energy of the neutron star is generally believed to power the radio emission of pulsars with spin periods ranging from 1.4 ms (Hessels et al. 2006) to 23.5 s (Tan et al. 2018). Most of the radio pulsars have spin periods $P \lesssim 1$ s and period derivatives $\dot{P} \lesssim 10^{-13}$ s s⁻¹ and span the region above the death line in the P – \dot{P} diagram (Ruderman & Sutherland 1975). The relatively slow radio pulsars of neutron-star spin periods in the ~ 1 –20 s range consist either of radio emitting transient anomalous X-ray pulsars (AXPs) or of radio pulsars with inferred surface magnetic dipole field strengths being close to or even exceeding the quantum critical value for electrons (Rea et al. 2012). The long-period radio pulsars such as PSR J0250+5854 are outnumbered compared to other pulsars partly because of the weak spin-down power which might be inadequate at sufficiently low \dot{P} and high P values to feed the radio emission mechanism in the pulsar’s magnetosphere and presumably also because of the selection effects such as low-frequency red noise and short dwell times making the detection of long-period sources difficult in most pulsar surveys (Tan et al. 2018).

The recent discovery of a low-frequency radio transient, namely GLEAM-X J162759.5-523504.3 exhibiting periodic pulsations with an extremely long period of ~ 1091 s has revealed the possible existence of a new class of radio pulsars as an extension of the usual radio pulsar population toward high P and \dot{P} values just above or near the pulsar death line in the P – \dot{P} diagram (Hurley-Walker et al. 2022). The radio pulses of GLEAM-X J162759.5-523504.3 are characterized by a stable high linear polarization pointing out the role of well ordered magnetic fields in the origin of radio emission. The typical range for

the pseudo-luminosity of the pulses, $L_\nu \sim 10^{21}$ – 10^{22} erg s⁻¹ Hz⁻¹, is higher by orders of magnitude than the pseudo-luminosity ranges of flare stars and white-dwarf binaries. The small fractional uncertainty in the measured pulse period strongly indicates the precision of the periodic emission. The search for the period derivative favours $\dot{P} > 0$, as expected for most of the radio pulsars (Hurley-Walker et al. 2022). It is therefore highly likely that the radio emitter in GLEAM-X J162759.5-523504.3 is indeed a slowly rotating neutron star and can therefore be seen as a new member of the long-period radio pulsar family.

For most of the radio pulsars, the radio luminosity L is only a small fraction of the pulsar’s spin-down power \dot{E} (also known as the spin-down luminosity). An anti-correlation holds between \dot{E} and the so-called radio efficiency $\epsilon \equiv L/\dot{E}$ because of the lack of any notable dependence of L on \dot{E} . The vast majority of radio pulsars including binary and millisecond pulsars, radio emitting AXPs, and young pulsars with pulsed high-energy radiation besides normal pulsars have radio efficiencies ranging from $\epsilon \sim 10^{-8}$ – 10^{-6} when the spin-down power is as high as $\dot{E} \sim 10^{36}$ – 10^{37} erg s⁻¹ to $\epsilon \sim 10^{-3}$ – 10^{-1} when $\dot{E} < 10^{31}$ erg s⁻¹ (Szary et al. 2014). For GLEAM-X J162759.5-523504.3, however, L has been claimed to exceed \dot{E} by at least three orders of magnitude in direct contrast with the behaviour of a rotation-powered radio pulsar. Instead, the source has been interpreted as a radio magnetar (Hurley-Walker et al. 2022) even though none of the radio emitting magnetar candidates had ever been observed with $\epsilon > 1$.

In this Letter, we calculate the radio luminosity of GLEAM-X J162759.5-523504.3 taking into account the dependence of the opening angle of the pulsar beam on the spin period of the neutron star and show that the spin-down power is not exceeded by the radio luminosity of the pulsar. We perform our calculations using the power-law

★ E-mail: mherkut@gmail.com

(PL) model first with a single PL index and then with two PL indices to describe the observed average weighted flux density in the 72–231 MHz frequency range. We also consider the dependence of the opening angle on the observing frequency. In all cases, we find the efficiency of the radio emission from GLEAM-X J162759.5-523504.3 to be consistent with the expected range of ϵ for pulsars with low \dot{E} .

2 RADIO LUMINOSITY OF THE PULSAR

2.1 Frequency-independent opening angle

Assuming that the opening angle of the pulsar beam does not depend on the observing frequency ν , the radio luminosity of a pulsar at a distance d can be written as

$$L = 4\pi d^2 \sin^2\left(\frac{\rho}{2}\right) \int_{\nu_{\min}}^{\nu_{\max}} S_p(\nu) d\nu, \quad (1)$$

where the so-called opening angle ρ is the angular radius of the pulsar's emission cone and the peak flux density $S_p(\nu)$ corresponds to the maximum intensity of the pulse profile (Lorimer & Kramer 2012). Here, $\sin^2(\rho/2)$ is known as the beaming fraction. The radio pulsars have been observed and probed within the frequency range determined by the integration limits in equation (1). Using the pulse duty cycle δ , the peak flux density S_p can be expressed in terms of the mean flux density S_m . For a flux density spectrum with a PL dependence on the observing frequency ν , we write the mean flux density,

$$S_m(\nu) = S_m(\nu_0) \left(\frac{\nu}{\nu_0}\right)^\alpha, \quad (2)$$

in terms of the reference frequency ν_0 and the PL index α . Substituting $S_p = S_m/\delta$ for the peak flux density and using equation (2), it follows from equation (1) that

$$L = 4\pi d^2 \sin^2\left(\frac{\rho}{2}\right) \left(\frac{\nu_{\max}^{\alpha+1} - \nu_{\min}^{\alpha+1}}{\alpha + 1}\right) \left[\frac{S_m(\nu_0)}{\nu_0^\alpha \delta}\right]. \quad (3)$$

Choosing the numerical values, which might be appropriate for most, if not all, radio pulsars, of the parameters in equation (3) to be $\delta = 0.04$, $\rho = 6^\circ$ (only for pulsars of spin period $P \sim 1$ s), $\alpha = -1.8$ (average value of the PL index for pulsar spectra above 100 MHz, see Maron et al. 2000), $\nu_{\min} = 10^7$ Hz, $\nu_{\max} = 10^{11}$ Hz, and $\nu_0 = 1.4$ GHz, the radio luminosity of a pulsar can be estimated from equation (3) as

$$L \approx 7.4 \times 10^{30} \left(\frac{d}{\text{kpc}}\right)^2 \left[\frac{S_m(1.4 \text{ GHz})}{\text{Jy}}\right] \text{erg s}^{-1} \quad (4)$$

(Lorimer & Kramer 2012). Note that the direct application of equation (4) to the specific case of GLEAM-X J162759.5-523504.3 is not a self-consistent approach to calculate the pulsar's radio luminosity and can be misleading when it comes to radio efficiency. The PL index inferred from the source spectrum is $\alpha = -1.16$ and should be used in equation (3) instead of equation (4), which in fact is obtained for $\alpha = -1.8$.

The peak flux density of pulses generated by GLEAM-X J162759.5-523504.3 at a reference frequency of 154 MHz was scaled by $\alpha = -1.16$ to the flux density at 1.4 GHz in equation (4) to find $L \approx 4 \times 10^{31}$ erg s $^{-1}$ (Hurley-Walker et al. 2022). There are several reasons of why such a high value of L , which is well above the spin-down power of the pulsar, was obtained: (i) the flux density at 1.4 GHz in equation (4) is the spin-period averaged value of the flux density and cannot be treated as the peak flux density unless the

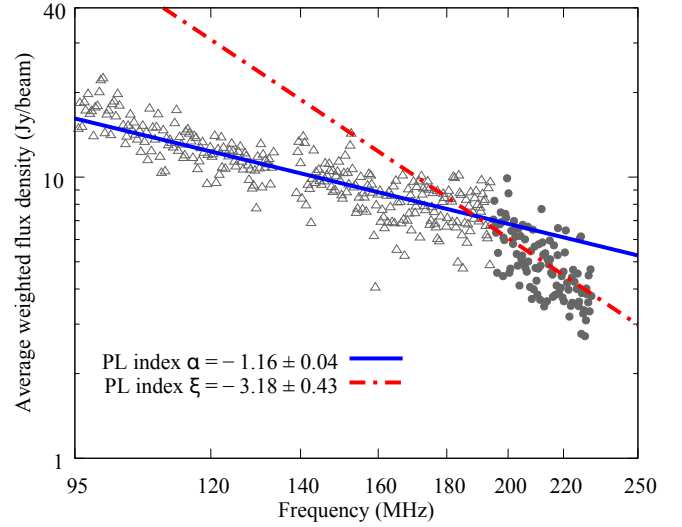


Figure 1. Spectral data fits for GLEAM-X J162759.5-523504.3 using PL models with different indices. Here, we plot the data in Hurley-Walker et al. (2022) without error bars for reasons of clarity. The low-frequency data between 95 and 195 MHz are shown as triangles. Filled circles denote the high-frequency tail of the data above 195 MHz. The best fit to the low-frequency part of the data is a PL with an index of $\alpha \approx -1.16$ (solid blue curve). The best fit to the high-frequency tail of the data between 195 and 231 MHz is another PL with an index of $\xi \approx -3.18$ (dotted-dashed red curve). See the text for the details about the PL fits in the plot.

whole expression in equation (4) is multiplied by the pulse duty cycle δ , i.e., $S_m = S_p \delta$, (ii) the flux in equation (4) is overestimated due to the scaling of the flux density by the incompatible PL indices, i.e., the flux is overestimated by $\alpha = -1.8(-1.16)$ at low(high) frequencies, and more importantly (iii) the luminosity estimate by equation (4) is based on the assumption that $P \sim 1$ s, which leads to the overestimation of the opening angle ρ and thus of L (see equation 3) for the long-period pulsar GLEAM-X J162759.5-523504.3.

Next, we obtain useful expressions for the radio luminosity of GLEAM-X J162759.5-523504.3 considering first a simple PL model of the source spectrum with a single index α (Section 2.1.1) and then a joint PL model of the same spectrum with two different PL indices, namely α and ξ (Section 2.1.2).

2.1.1 Spectrum with a single PL index

The PL model fit to the average weighted flux-density data between 95 and 195 MHz yielded a PL spectral index of $\alpha = -1.16 \pm 0.04$, which in turn was proposed to represent the extended data between 72 and 231 MHz (Hurley-Walker et al. 2022). The best fit to the spectral data between 95 and 195 MHz is shown in Fig. 1.

We calculate the radio luminosity of the pulsar using the expression in equation (3) to the extent that the whole spectral data, including the high-frequency tail, can be accounted for using a PL model with a single index $\alpha \approx -1.16$ (solid blue curve in Fig. 1). The pulsar's radio luminosity (see equation 3) can be written in terms of the peak flux density as

$$L = 4\pi d^2 \sin^2\left(\frac{\rho}{2}\right) \left(\frac{\nu_{\max}^{\alpha+1} - \nu_{\min}^{\alpha+1}}{\alpha + 1}\right) \left[\frac{S_p(\nu_0)}{\nu_0^\alpha}\right], \quad (5)$$

remembering that $S_p = S_m/\delta$. For GLEAM-X J162759.5-523504.3,

the peak flux density at the reference frequency was reported to be $S_p(154 \text{ MHz}) = 45 \text{ Jy}$ (see Hurley-Walker et al. 2022).

2.1.2 Spectrum with two PL indices

The average weighted flux-density spectrum was fitted by a power law with an index of $\alpha = -1.16 \pm 0.04$ using the least-squares method to find the best fit to the data between 95 and 195 MHz (Hurley-Walker et al. 2022). The PL fit with an index of $\alpha \simeq -1.16$ may, however, overestimate the flux density at the high-frequency tail of the spectrum. The sharp downturn in the flux density at high frequencies ($> 195 \text{ MHz}$) is noticeable from Fig. 1. It is highly likely that a steeper PL fit to the remaining data between 195 and 231 MHz would represent the spectral data extrapolated toward higher frequencies better than a flatter PL with an index of ~ -1.16 .

We use the nonlinear least-squares Marquardt-Levenberg algorithm to perform a PL fit to the flux-density data in the 195–231 MHz range. The best fit to the high-frequency data with a reduced χ^2 of ~ 1.12 is obtained as a PL with an index of $\xi = -3.18 \pm 0.43$ (dotted-dashed red curve in Fig. 1). Note that the two PL model fits with indices $\alpha \simeq -1.16$ and $\xi \simeq -3.18$ describe the low and high frequency domains, respectively, and intersect at a frequency $\nu_1 \simeq 189 \text{ MHz}$ (Fig. 1). Next, we consider the frequency of intersection, ν_1 , as a limiting point where the spectrum switches the frequency dependence from a relatively flat to a steep PL and therefore as an intermediate limit of the integral in equation (1) to calculate the radio luminosity of the pulsar.

For a spectrum of frequency dependence depicted by two different PL indices, the mean flux density can be expressed as

$$S_m(\nu) = \begin{cases} S_m(\nu_0) (\nu/\nu_0)^\alpha, & \text{for } \nu \leq \nu_1; \\ S_m(\nu_1) (\nu/\nu_1)^\xi, & \text{for } \nu \geq \nu_1. \end{cases} \quad (6)$$

Here, the continuity at ν_1 can only be satisfied if

$$S_m(\nu_1) = S_m(\nu_0) \left(\frac{\nu_1}{\nu_0} \right)^\alpha. \quad (7)$$

Using equations (6) and (7) and remembering that $S_p = S_m/\delta$, it follows from equation (1) that

$$L = L(\nu \leq \nu_1) + L(\nu \geq \nu_1), \quad (8)$$

where

$$L(\nu \leq \nu_1) = 4\pi d^2 \sin^2 \left(\frac{\rho}{2} \right) \left(\frac{\nu_1^{\alpha+1} - \nu_{\min}^{\alpha+1}}{\alpha+1} \right) \left[\frac{S_p(\nu_0)}{\nu_0^\alpha} \right] \quad (9)$$

and

$$L(\nu \geq \nu_1) = 4\pi d^2 \sin^2 \left(\frac{\rho}{2} \right) \left(\frac{\nu_{\max}^{\xi+1} - \nu_1^{\xi+1}}{\xi+1} \right) \left[\frac{\nu_1^{\alpha-\xi} S_p(\nu_0)}{\nu_0^\alpha} \right]. \quad (10)$$

As expected, equation (8) is reduced back to equation (5) when $\xi = \alpha$.

2.1.3 Spin-period dependence of the opening angle

The angular radius of the pulsar beam, ρ , also known as the opening angle of the pulsar's emission cone, was found to depend on the spin period of the pulsar. The analysis of the emission-cone geometry for a pulsar population revealed the $P^{-1/2}$ dependence of the opening angle for both the so-called inner and outer cones of the radio emission. The relatively long-period pulsars seem to prefer the outer cone with

$$\rho \simeq 6^\circ \left(\frac{P}{\text{s}} \right)^{-1/2}, \quad (11)$$

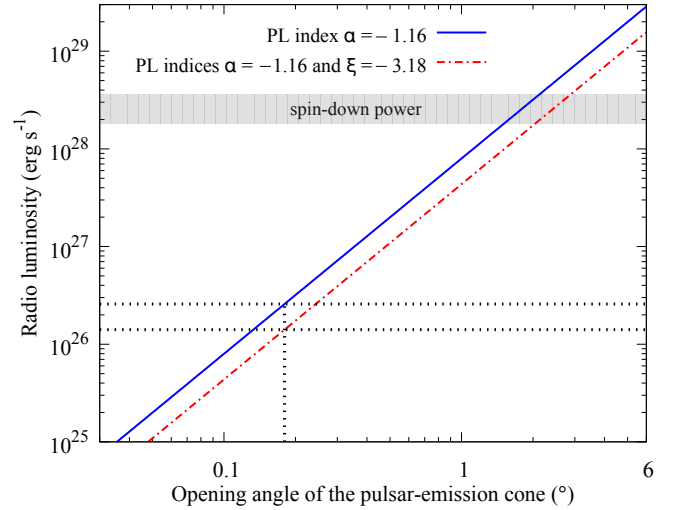


Figure 2. Radio luminosity of GLEAM-X J162759.5-523504.3 as a function of the opening angle ρ , which is treated here as independent of ν . The radio luminosity corresponding to the spectrum with a single PL index $\alpha = -1.16$ (equation 5) is shown by the solid blue curve. The spectrum described by the two PL indices, $\alpha = -1.16$ and $\xi = -3.18$, yields the radio luminosity (equation 8) shown by the dotted-dashed red curve. The two possible radio luminosity values of GLEAM-X J162759.5-523504.3 (horizontal dotted lines) are estimated by the solid blue and dotted-dashed red curves at $\rho \simeq 0.18^\circ$ (see Section 2.1.3), as shown by the vertical dotted line. The interval for the spin-down power of the pulsar is displayed by the horizontal grey stripe. See the text (Section 3) for the specific values of the radio luminosity and the spin-down power.

where P is the neutron-star spin period (Rankin 1993; Gil et al. 1993). Note that $\rho \simeq 6^\circ$ only for pulsars of spin period $\sim 1 \text{ s}$. For GLEAM-X J162759.5-523504.3, however, $P \simeq 1091 \text{ s}$ and therefore $\rho \simeq 0.18^\circ$ according to equation (11).

For a pulsar's magnetosphere of dipolar field geometry in polar coordinates (r, θ) , $r/\sin^2 \theta$ is a constant and can be written for the last open field line at the light-cylinder radius as

$$\frac{r}{\sin^2 \theta} = \frac{cP}{2\pi}, \quad (12)$$

where c is the speed of light. For regions close to the magnetic axis of the pulsar, that is, for sufficiently small values of θ and ρ (i.e., $\theta < 20^\circ$ and $\rho < 30^\circ$), the relation between the opening angle of the emission cone, ρ , and the polar angle of the emission point on the field line, θ , is approximated by $\rho/\theta \simeq 3/2$ (Gangadhara & Gupta 2001). For small angles, equation (12) can then be used for finding the relation between ρ and the emission height r as

$$\rho = 1.24 \left(\frac{r}{10 \text{ km}} \right)^{1/2} \left(\frac{P}{\text{s}} \right)^{-1/2} \quad (13)$$

(see also Lorimer & Kramer 2012). If the emission height r in the pulsar's magnetosphere is independent of the spin period as proposed by Rankin (1993), the empirical relation given by equation (11) can be seen to be in agreement with equation (13).

The subsequent studies relying on the measurements of pulse width, however, have revealed that the emission height r depends on both the observing frequency ν and the spin parameters of the pulsar such as the spin period P and its derivative \dot{P} (Kijak & Gil 1997, 2003). The opening angle is then expected in line with equation (13) to depend on ν as well. Next, we consider the frequency-dependent

opening angle $\rho(\nu)$ and derive, in a similar way to frequency-independent ρ (Sections 2.1.1 and 2.1.2), the luminosity expressions based on the source spectrum to be modelled first with a single PL index and then with two PL indices.

2.2 Frequency-dependent opening angle

The empirical relationship for the radio emission height in a pulsar magnetosphere can be written in terms of the observing frequency ν and the spin parameters P and \dot{P} as

$$\frac{r}{10 \text{ km}} \simeq 40 \left(\frac{\nu}{\nu_s} \right)^\beta \left(\frac{\dot{P}}{10^{-15} \text{ s s}^{-1}} \right)^{0.07} \left(\frac{P}{\text{s}} \right)^{0.30}, \quad (14)$$

where $\beta \simeq -0.26$ and $\nu_s = 1 \text{ GHz}$ is a scaling frequency (Kijak & Gil 2003). Note that the radio emission at relatively low frequencies is expected to occur at higher altitudes and therefore with larger opening angles for the pulsar beam (equations 13 and 14).

The dependence of the opening angle on the observing frequency can be taken into account when the radio luminosity of a pulsar at a distance d ,

$$L = 4\pi d^2 \int_{\nu_{\min}}^{\nu_{\max}} \sin^2 \left[\frac{\rho(\nu)}{2} \right] S_p(\nu) d\nu, \quad (15)$$

is calculated through the integration of the peak flux density weighted by the beaming fraction as ν changes. For sufficiently small values of ρ (see Section 2.1.3), equation (15) can be expressed to a very good approximation as

$$L \simeq \pi d^2 \int_{\nu_{\min}}^{\nu_{\max}} \rho^2(\nu) S_p(\nu) d\nu. \quad (16)$$

Here, ρ is measured in radians.

2.2.1 Spectrum with a single PL index

Using equation (2) with $S_m = S_p \delta$, it follows from equations (13), (14), and (16) that

$$L = 4\pi d^2 f(P, \dot{P}) \left(\frac{\nu_{\max}^{\alpha+\beta+1} - \nu_{\min}^{\alpha+\beta+1}}{\alpha + \beta + 1} \right) \left[\frac{S_p(\nu_0)}{\nu_0^\alpha \nu_s^\beta} \right], \quad (17)$$

where the dimensionless function of P and \dot{P} can be written as

$$f(P, \dot{P}) \simeq 4.68 \times 10^{-3} \left(\frac{\dot{P}}{10^{-15} \text{ s s}^{-1}} \right)^{0.07} \left(\frac{P}{\text{s}} \right)^{-0.7}. \quad (18)$$

The pulsar-luminosity expression in equation (17) is analogous to that in equation (5) when β vanishes.

2.2.2 Spectrum with two PL indices

Now, we use equations (6) and (7) with $S_m = S_p \delta$ and obtain, in analogy with equation (8), the pulsar luminosity,

$$L = 4\pi d^2 [F(\nu \leq \nu_1) + F(\nu \geq \nu_1)], \quad (19)$$

from equations (13), (14), and (16) such that

$$F(\nu \leq \nu_1) = f(P, \dot{P}) \left(\frac{\nu_{\max}^{\alpha+\beta+1} - \nu_{\min}^{\alpha+\beta+1}}{\alpha + \beta + 1} \right) \left[\frac{S_p(\nu_0)}{\nu_0^\alpha \nu_s^\beta} \right] \quad (20)$$

and

$$F(\nu \geq \nu_1) = f(P, \dot{P}) \left(\frac{\nu_{\max}^{\xi+\beta+1} - \nu_1^{\xi+\beta+1}}{\xi + \beta + 1} \right) \left[\frac{\nu_1^{\alpha-\xi} S_p(\nu_0)}{\nu_0^\alpha \nu_s^\beta} \right]. \quad (21)$$

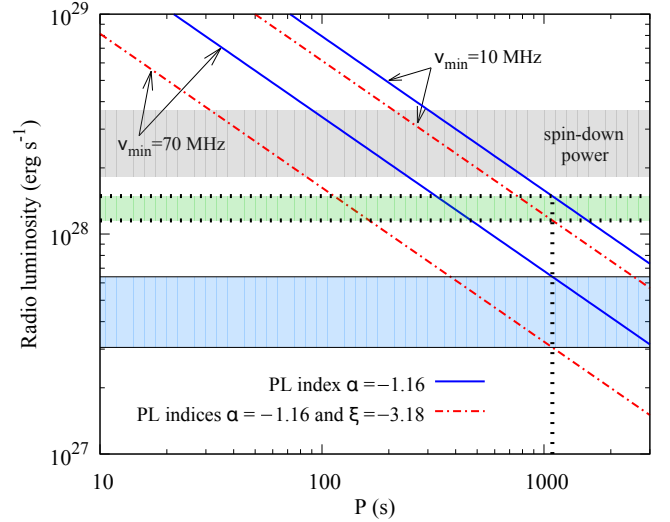


Figure 3. Radio luminosity of GLEAM-X J162759.5-523504.3 as a function of the pulsar’s spin period P for an opening angle that depends on ν . The two sets of radio luminosity curves (solid blue and dotted-dashed red curves) are obtained for the two different values of the minimum observing frequency, namely for $\nu_{\min} = 10 \text{ MHz}$ and 70 MHz . The radio luminosity for a spectrum with a single PL index $\alpha = -1.16$ (equation 17) is shown by the solid blue curves. The radio luminosity for a spectrum with two PL indices, $\alpha = -1.16$ and $\xi = -3.18$ (equation 19), is plotted by the dotted-dashed red curves. The two possible sets of radio luminosity values for GLEAM-X J162759.5-523504.3, which are shown by the horizontal dotted and solid lines as boundaries of green and blue stripes, are estimated at $P \simeq 1091 \text{ s}$ by the solid blue and dotted-dashed red curves when $\nu_{\min} = 10 \text{ MHz}$ and 70 MHz , respectively. The interval for the spin-down power of the pulsar is displayed by the horizontal grey stripe as in Fig. 2. See the text (Section 3) for the specific values of the radio luminosity and the spin-down power.

Note that equation (19) can be reduced back to equation (17) for $\xi = \alpha$.

Next, we present our results concerning the luminosity estimate of GLEAM-X J162759.5-523504.3 in radio for both cases of frequency-independent and frequency-dependent opening angle.

3 RESULTS & DISCUSSION

First, we consider the relations derived from the presumption of frequency-independent opening angle (Section 2.1). We employ equation (5) to estimate the radio luminosity of GLEAM-X J162759.5-523504.3 to the extent that the whole spectral data can be described by a single PL index $\alpha \simeq -1.16$ in line with the former suggestion by Hurley-Walker et al. (2022). We then use equation (8) to calculate the radio luminosity of GLEAM-X J162759.5-523504.3 based on a more accurate modelling of the observed spectrum in terms of the two PL indices, $\alpha \simeq -1.16$ and $\xi \simeq -3.18$ to account for the low ($\nu < 195 \text{ MHz}$) and high ($\nu > 195 \text{ MHz}$) frequency data, respectively (see Fig. 1).

Besides the wide frequency range determined by $\nu_{\min} \simeq 10^7 \text{ Hz}$ and $\nu_{\max} \simeq 10^{11} \text{ Hz}$ for pulsar study and detection (Lorimer & Kramer 2012), the numerical values of the parameters we choose in equation (5) and equations (8)–(10) are appropriate to GLEAM-X J162759.5-523504.3. We set $\nu_0 = 154 \text{ MHz}$, $S_p(\nu_0) = 45 \text{ Jy}$, $\alpha = -1.16$, $\xi = -3.18$, and $\nu_1 = 189 \text{ MHz}$. For a source distance of $d \simeq 1.3 \text{ kpc}$ (Hurley-Walker et al. 2022), the possible value of the

opening angle, i.e., $\rho \simeq 0^\circ.18$ (see Section 2.1.3), for $P \simeq 1091$ s implies a radio luminosity of $L \simeq 2.6 \times 10^{26}$ erg s $^{-1}$ for a spectrum with a single PL index and $L \simeq 1.4 \times 10^{26}$ erg s $^{-1}$ for a spectrum with two PL indices (Fig. 2).

Even if ρ is treated as a frequency-independent parameter—the direct application of equation (4) by Hurley-Walker et al. (2022) to the radio luminosity of GLEAM-X J162759.5-523504.3 is a typical example—it cannot be regarded as a period-independent parameter. As seen from Fig. 2, the radio luminosity of GLEAM-X J162759.5-523504.3 exceeds the spin-down power of the pulsar,

$$\dot{E} \simeq 1.82 \times 10^{28} I_{45} \left(\frac{\dot{P}}{6 \times 10^{-10} \text{ s s}^{-1}} \right) \left(\frac{P}{1091 \text{ s}} \right)^{-3} \text{ erg s}^{-1}, \quad (22)$$

only for $\rho \gtrsim 2^\circ$, that is, for $P < 9$ s (see equation 11). Here, I_{45} is the neutron-star moment of inertia measured in units of 10^{45} g cm 2 . The upper limit for the measured period derivative, $\dot{P}_{\text{max}} = 1.2 \times 10^{-9}$ s s $^{-1}$ was found to be twice the best-fit value we use in equation (22) for \dot{P} (Hurley-Walker et al. 2022). The maximum spin-down power of GLEAM-X J162759.5-523504.3 is then $\dot{E}_{\text{max}} \simeq 3.64 \times 10^{28}$ erg s $^{-1}$. The grey stripes plotted in Fig. 2 as well as in Fig. 3 are determined by these best-fit and maximum \dot{E} values, which are greater by a factor of π than the spin-down luminosity values found by Hurley-Walker et al. (2022) who probably missed such a factor while computing the spin-down power. As a long-period pulsar, GLEAM-X J162759.5-523504.3 is expected to have a fainter radio luminosity with respect to the spin-down power than an ordinary pulsar of $P \sim 1$ s with $\rho \sim 6^\circ$ (Fig. 2).

In a physically more plausible scenario, however, ρ increases with decreasing ν as suggested by equations (13) and (14) and we need to consider the relations based on the frequency-dependent opening angle (Section 2.2). We basically use equations (17) and (19) to estimate the radio luminosity of GLEAM-X J162759.5-523504.3 for a spectrum with a single PL index and a spectrum with two PL indices, respectively.

In addition to all numerical values we have chosen in the case of frequency-independent ρ for the parameters such as ν_0 , $S_p(\nu_0)$, α , ξ , ν_1 , and d , we set $\nu_s = 1$ GHz, $\beta = -0.26$, and $\dot{P} = 6 \times 10^{-10}$ s s $^{-1}$ to obtain the luminosity estimate of GLEAM-X J162759.5-523504.3, as shown in Fig. 3. The luminosity curves are plotted for two different values of ν_{min} to see the contribution of ever increasing ρ at low frequencies to the total radio output of the source. In the absence of any spectral data of GLEAM-X J162759.5-523504.3 at frequencies below 70 MHz, we consider two possibilities: (i) the radio emission might be extended to very low frequencies, i.e., $\nu_{\text{min}} \simeq 10$ MHz, but might have suffered from interstellar and ionospheric scintillation or (ii) the source is not radio luminous at all at frequencies less than $\nu_{\text{min}} \simeq 70$ MHz. In Fig. 3, the curves labelled with $\nu_{\text{min}} = 10$ MHz yield the highest possible radio luminosity values at $P \simeq 1091$ s and yet the spin-down power is not exceeded. We read $L \simeq 1.5 \times 10^{28}$ erg s $^{-1}$ for a single PL index and $L \simeq 1.2 \times 10^{28}$ erg s $^{-1}$ for double PL indices. The radio luminosities estimated by the curves labelled with $\nu_{\text{min}} = 70$ MHz are $L \simeq 6.4 \times 10^{27}$ erg s $^{-1}$ and $L \simeq 3.0 \times 10^{27}$ erg s $^{-1}$ for a single PL index and double PL indices, respectively (Fig. 3).

For a radio pulsar of P exceeding 10^3 s such as GLEAM-X J162759.5-523504.3, the opening angles are expected to attain values as small as $\rho \simeq 0^\circ.18$ for the frequency-independent case. Albeit higher, the opening angle in equation (16) for the frequency-dependent case can be seen from equations (13) and (14) to vary between $\rho_{\text{max}} \simeq 2^\circ$ and $\rho_{\text{min}} \simeq 0^\circ.6$ at $\nu_{\text{min}} = 10^7$ Hz and $\nu_{\text{max}} = 10^{11}$ Hz, respectively. There is, however, a lower limit for ρ due to relativistic beaming and the realization of such small ρ

values must be checked. Indeed, $\rho > \Delta\rho$, where $\Delta\rho \simeq \gamma^{-1}$ is the opening angle of the curvature-radiation cone generated by a localized source of ultra-relativistic particles of Lorentz factor γ moving along dipolar magnetic field lines. The typical value of γ in a pulsar magnetosphere is of the order of 100, i.e., $10^2 < \gamma < 10^3$ (Gil 1983; Gangadhara 2004; Gil & Melikidze 2005), yielding the $0^\circ.57$ – $0^\circ.057$ range for $\Delta\rho$. Our range for the frequency-dependent ρ values is therefore already plausible. The smallest value of the lower limit for γ can be estimated using equation (6) in Gil (1983). Substituting 220 MHz for the maximum emitted frequency, 10 or 100 for the maximum coherence parameter κ , and 1227 for the $f = r_{\text{min}}/10$ km parameter corresponding to $\nu = 220$ MHz (see equation 14) together with other parameters being appropriate to GLEAM-X J162759.5-523504.3, we obtain the lower limits for γ as $\gamma_{\text{min}} \simeq 696$ when $\kappa = 10$ and $\gamma_{\text{min}} \simeq 323$ when $\kappa = 100$. The corresponding $\Delta\rho$ values are $< 0^\circ.08$ and $0^\circ.18$, respectively. Even if ρ slightly exceeds $0^\circ.18$ for smaller values of γ , the radio emission can still be rotationally powered since $L < \dot{E}$ for $\rho \lesssim 2^\circ$ (see Fig. 2).

In summary, the highest possible radio luminosity of GLEAM-X J162759.5-523504.3 based on the maximum peak flux density of ~ 45 Jy observed at $\nu_0 = 154$ MHz does not exceed the pulsar's spin-down power of $\sim 1.8 \times 10^{28}$ erg s $^{-1}$. It is rather highly likely that the source is a pulsating neutron star with a radio efficiency $\epsilon \gtrsim 0.1$ as expected from the long-period members of the pulsar population with sufficiently low spin-down power (see Section 1). The opening angles of such long-period pulsars are extremely small at relatively high frequencies making the detection of such transient sources more likely at low frequencies.

ACKNOWLEDGEMENTS

I thank O. Çatmabacak and Ö. Çatmabacak for inspiring discussions and useful comments.

DATA AVAILABILITY

The data used in this article are already available in Hurley-Walker et al. (2022).

REFERENCES

- Gangadhara R. T., 2004, *ApJ*, **609**, 335
 Gangadhara R. T., Gupta Y., 2001, *ApJ*, **555**, 31
 Gil J., 1983, *A&A*, **123**, 7
 Gil J., Melikidze G. I., 2005, *A&A*, **432**, L61
 Gil J. A., Kijak J., Seiradakis J. H., 1993, *A&A*, **272**, 268
 Hessels J. W. T., Ransom S. M., Stairs I. H., Freire P. C. C., Kaspi V. M., Camilo F., 2006, *Science*, **311**, 1901
 Hurley-Walker N., et al., 2022, *Nature*, **601**, 526
 Kijak J., Gil J., 1997, *MNRAS*, **288**, 631
 Kijak J., Gil J., 2003, *A&A*, **397**, 969
 Lorimer D. R., Kramer M., 2012, *Handbook of Pulsar Astronomy*. Cambridge University Press
 Maron O., Kijak J., Kramer M., Wielebinski R., 2000, *A&AS*, **147**, 195
 Rankin J. M., 1993, *ApJ*, **405**, 285
 Rea N., Pons J. A., Torres D. F., Turolla R., 2012, *ApJ*, **748**, L12
 Ruderman M. A., Sutherland P. G., 1975, *ApJ*, **196**, 51
 Szary A., Zhang B., Melikidze G. I., Gil J., Xu R.-X., 2014, *ApJ*, **784**, 59
 Tan C. M., et al., 2018, *ApJ*, **866**, 54

This paper has been typeset from a \LaTeX file prepared by the author.